




Cite this: *RSC Adv.*, 2017, 7, 53439

# A novel self-assembled supramolecular sensor based on thiophene-functionalized imidazophenazine for dual-channel detection of Ag<sup>+</sup> in an aqueous solution†

Hai-Xiong Shi, Wen-Ting Li, Qiao Li, Hai-Li Zhang, You-Ming Zhang,  Tai-Bao Wei, \* Qi Lin  and Hong Yao

Herein, a novel self-assembled supramolecular sensor (**S1**) based on thiophene-functionalized imidazophenazine for Ag<sup>+</sup> was designed and synthesized. It showed dual-channel detection properties for Ag<sup>+</sup> based on the competitive mechanism of supramolecular self-assembly with high sensitivity and selectivity even in the presence of other metal ions. Its detection limit for Ag<sup>+</sup> is  $8.18 \times 10^{-9}$  M. Upon the addition of Ag<sup>+</sup>, the solution changes from yellow to light purple and the fluorescence is quenched. Furthermore, the sensing mechanism between Ag<sup>+</sup> and **S1** is investigated via IR and <sup>1</sup>H NMR spectroscopy, mass spectrometry, and density functional theory calculations.

Received 29th August 2017  
Accepted 7th November 2017

DOI: 10.1039/c7ra09597j

rsc.li/rsc-advances

## Introduction

With the development of modern industry, increasing industrial emissions containing metal ions have caused serious water pollution, which affects food and agriculture and further threatens human health and the environment.<sup>1</sup> Among the important metal ions, silver has attracted extensive attention due to its wide applications in the fields of electricity, photography, imaging, and pharmacy.<sup>2</sup> In fact, trace amounts of silver ions can control bacteria breeding or rehabilitate and reconstruct essential human tissue.<sup>3</sup> However, as is well known, excess silver ions can inactivate sulfhydryl enzymes; on the other hand, silver ions can combine with amine, imidazole, and carboxyl groups of various metabolites, such as high molecular weight protein and metallothionein, in the tissue of the cytosol fraction, resulting in harmful effects to humans.<sup>4</sup> Thus, the maximum bearable concentration of Ag(I) issued by the World Health Organization (WHO) is 0.5 μM in drinking water.<sup>5</sup>

Considering the importance of Ag(I) in industrial production and in daily life, the development of techniques for sensing and monitoring Ag(I) is in great demand. There are various available methods to monitor Ag<sup>+</sup>, such as electrothermal atomic absorption spectrometry (ETAAS), voltammetry, inductively coupled plasma atomic emission spectrometry (ICP-AES), inductively coupled plasma mass spectroscopy (ICP-MS), and

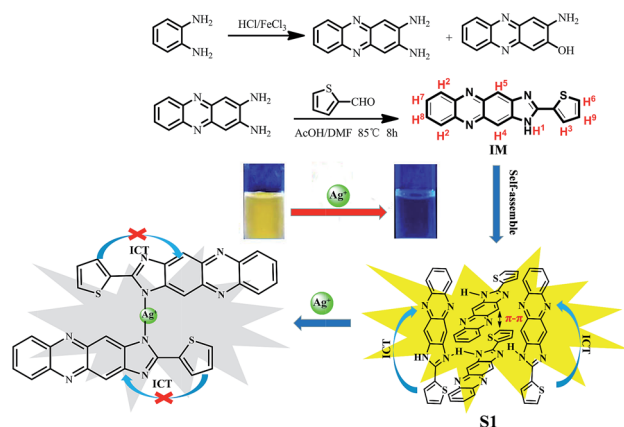
potentiometry.<sup>6</sup> However, most of them are expensive, time-consuming, or unsuitable for on-site and real-time monitoring. Therefore, the development of fast, efficient, sensitive, and selective methods for the detection of Ag<sup>+</sup> is necessary for both the environment and human health.<sup>7</sup> In comparison, fluorescence techniques exhibit attractive advantages, such as high selectivity and sensitivity, real-time detection, practical-simple sample preparation, and great potential in high throughput detection of Ag<sup>+</sup> on-site. However, some of these probes suffer from serious drawbacks such as complicated synthesis procedures and poor solubility, sensitivity, and selectivity in aqueous media.<sup>8</sup> Due to the efforts of researchers, numerous Ag<sup>+</sup> sensors with good properties have been reported. However, most of them exhibit ultraviolet or fluorescent single channel recognition or are less selective.<sup>9</sup> Moreover, it is worthwhile to note that sensors for the detection of Ag<sup>+</sup> in aqueous systems are relatively scarce although Ag<sup>+</sup> usually exists in water or sewerage. Consequently, the design and synthesis of colorimetric and fluorescent chemosensors with high sensitivity and selectivity for the quantification of Ag<sup>+</sup> in aqueous media via a simple reaction is still an intriguing area of research.<sup>10</sup>

In view of this and based on our previous research in host-guest chemistry,<sup>11</sup> we designed and synthesized a sensor molecule **IM** (Scheme 1) based on thiophene-functionalized imidazophenazine via a simple reaction; this sensor could self-assemble into a supramolecular system and form a supramolecular chemosensor **S1**. This sensor combines the phenazine fluorescent signaling subunit, which has attracted extensive attention due to its excellent photophysical properties. In addition, among the different fluorogens, it is very sensitive to

Key Laboratory of Eco-Environment-Related Polymer Materials, Ministry of Education of China, Key Laboratory of Polymer Materials of Gansu Province, College of Chemistry and Chemical Engineering, Northwest Normal University, Lanzhou, Gansu, 730070, P. R. China. E-mail: weitaobao@126.com

† Electronic supplementary information (ESI) available: Experimental details, synthesis of **S1**, NMR spectra, and other materials. See DOI: 10.1039/c7ra09597j





**Scheme 1** Synthesis of the compound IM and the proposed possible mechanism of **S1** bonding with  $\text{Ag}^+$ .

conformational changes.<sup>12</sup> Consequently, phenazines are ideal platforms for the development of cation, anion, and neutral molecule recognition platforms. Moreover, there are only a few reports on ion recognition in host–guest chemistry. Compared to some  $\text{Ag}^+$  sensors reported in previous studies, the  $\text{Ag}^+$  sensor reported herein is a self-assembled supramolecular sensor (**S1**). The  $\text{Ag}^+$  sensing mechanism is based on a competition between self-assembly of the sensor molecules and  $\text{Ag}^+$  coordination with the sensor molecules. This novel competitive mechanism provides the **S1** sensor with better  $\text{Ag}^+$  detection sensitivity. The detection limit of **S1** for  $\text{Ag}^+$  is  $8.18 \times 10^{-9}$  M, which is lower than that reported in some previous studies.<sup>8</sup> Therefore, **S1** is utilized as a supramolecular self-assembled sensor to study the recognition performance of  $\text{Ag}^+$ .

## Results and discussion

To investigate the  $\text{Ag}^+$  recognition abilities of the **S1** sensor in an aqueous solution, we performed a series of host–guest recognition experiments. The recognition profiles of the chemosensor **S1** towards various metal ions, including  $\text{Fe}^{3+}$ ,  $\text{Hg}^{2+}$ ,  $\text{Ag}^+$ ,  $\text{Ca}^{2+}$ ,  $\text{Cu}^{2+}$ ,  $\text{Co}^{2+}$ ,  $\text{Ni}^{2+}$ ,  $\text{Cd}^{2+}$ ,  $\text{Pb}^{2+}$ ,  $\text{Zn}^{2+}$ ,  $\text{Cr}^{3+}$ , and  $\text{Mg}^{2+}$ , were primarily investigated using UV-vis spectroscopy and fluorescence spectroscopy in a DMSO/water (v:v = 1 : 1, buffered with HEPES pH = 7.2) solution.

As shown in Fig. 1, the sensor immediately responded with obvious color changes (from yellow to light purple) when  $\text{Ag}^+$  was added to the **S1** solution at room temperature. In the corresponding UV-vis spectra, the strength of the absorption peak at 413 nm decreased, and the peak red-shifted to 376 nm (Fig. S1†). However, yellow fluorescence with one emission band centered at 547 nm appeared when the **S1** sensor solution was excited at 400 nm. The fluorescence intensity of the peak at 547 nm sharply decreased with the addition of the  $\text{Ag}^+$  solution. No significant UV-vis or fluorescence spectra changes were observed when solutions of other cations (such as  $\text{Fe}^{3+}$ ,  $\text{Hg}^{2+}$ ,  $\text{Ca}^{2+}$ ,  $\text{Cu}^{2+}$ ,  $\text{Co}^{2+}$ ,  $\text{Ni}^{2+}$ ,  $\text{Cd}^{2+}$ ,  $\text{Pb}^{2+}$ ,  $\text{Zn}^{2+}$ ,  $\text{Cr}^{3+}$ , and  $\text{Mg}^{2+}$ ) were added to the **S1** sensor solution.

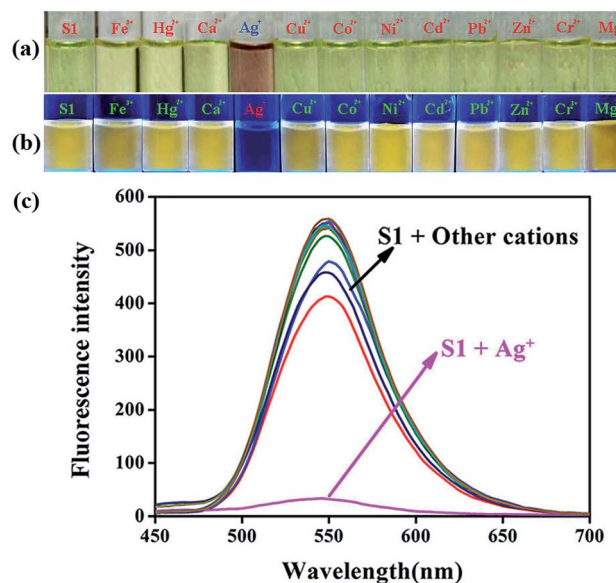


**Fig. 1** An image of **S1** upon the addition of 10 equiv. of various cations in DMSO/ $\text{H}_2\text{O}$  (v:v = 1 : 1, buffered with HEPES pH = 7.2), which was taken under (a) visible light and (b) UV-lamp (365 nm) at room temperature. (c) Fluorescence spectral responses in DMSO/ $\text{H}_2\text{O}$  (v:v = 1 : 1, buffered with HEPES pH = 7.2) of **S1** ( $2.0 \times 10^{-5}$  M) upon the addition of different cations (10 equiv.).

Subsequently, we further investigated the supramolecular sensor **S1** recognition for  $\text{Pd}^{2+}$ , as shown in Fig. S2 and S3;† however, **S1** could not sense  $\text{Pd}^{2+}$ . These results confirmed that the self-assembly supramolecular sensor **S1** could sense  $\text{Ag}^+$  with high sensitivity and selectivity.

The specific selectivity of a sensor towards an analyte in the presence of other competitive species is important. To explore the utility of the **S1** sensor as an ion-selective chemosensor for  $\text{Ag}^+$ , competitive experiments were carried out in the presence of 10 equiv. of  $\text{Ag}^+$  and 10 equiv. of  $\text{Fe}^{3+}$ ,  $\text{Hg}^{2+}$ ,  $\text{Ca}^{2+}$ ,  $\text{Cu}^{2+}$ ,  $\text{Co}^{2+}$ ,  $\text{Ni}^{2+}$ ,  $\text{Cd}^{2+}$ ,  $\text{Pb}^{2+}$ ,  $\text{Zn}^{2+}$ ,  $\text{Cr}^{3+}$ , and  $\text{Mg}^{2+}$  metal ions in DMSO/water (v:v = 1 : 1, buffered with HEPES pH = 7.2) binary solutions of the **S1** sensor (Fig. 2 and S4†). From the bar diagram, it was observed that none of these ions induced any significant change in the fluorescence and UV-vis absorbance spectrum of the sensor. Therefore, it is clear that the interference of other ions is negligible during the detection of  $\text{Ag}^+$ . These results further suggested that **S1** could be used as a sensor for  $\text{Ag}^+$  over a wide range of cations. Thus, **S1** could selectively and instantly (dual-channel) detect  $\text{Ag}^+$  in DMSO/water (v:v = 1 : 1, buffered with HEPES pH = 7.2).

To evaluate the  $\text{Ag}^+$ -responsive nature of **S1**, fluorescence and UV-vis absorbance titrations with  $\text{Ag}^+$  at varying concentrations were conducted. As shown in Fig. 3, upon the addition of  $\text{Ag}^+$  to the **S1** sensor, the emission peak at 547 nm gradually diminished, and the fluorescence of **S1** was almost quenched by 18.0 equiv. of  $\text{Ag}^+$  ions. In the UV-vis spectra (Fig. 4), the initial absorption peak at 413 nm gradually decreased, and simultaneously, a broad shoulder peak appeared at 530 nm and an isosbestic point at 495 nm was clearly observed. This should be attributed to the damage of intramolecular hydrogen-bonding



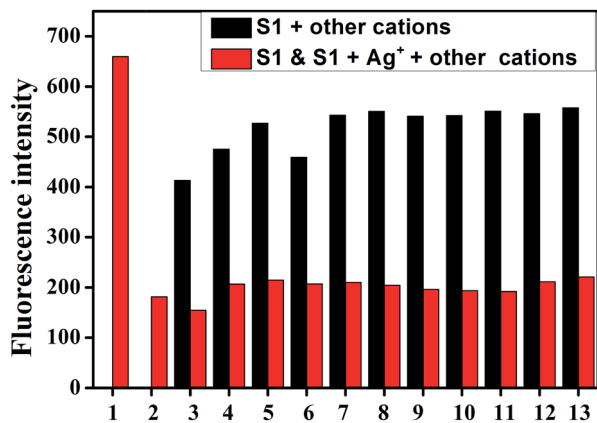


Fig. 2 Fluorescent emission ( $\lambda_{\text{ex}} = 400$  nm) spectra of **S1** ( $2 \times 10^{-5}$  M) and  $\text{Ag}^+$  (10 equiv.) in the presence of various competing cations in DMSO/ $\text{H}_2\text{O}$  (v:v = 1 : 1, buffered with HEPES pH = 7.2) solution. From 1 to 13: **S1**, **S1** +  $\text{Ag}^+$ , **S1** +  $\text{Ag}^+$  +  $\text{Fe}^{3+}$ , **S1** +  $\text{Ag}^+$  +  $\text{Ca}^{2+}$ , **S1** +  $\text{Ag}^+$  +  $\text{Cu}^{2+}$ , **S1** +  $\text{Ag}^+$  +  $\text{Co}^{2+}$ , **S1** +  $\text{Ag}^+$  +  $\text{Ni}^{2+}$ , **S1** +  $\text{Ag}^+$  +  $\text{Cd}^{2+}$ , **S1** +  $\text{Ag}^+$  +  $\text{Pb}^{2+}$ , **S1** +  $\text{Ag}^+$  +  $\text{Zn}^{2+}$ , **S1** +  $\text{Ag}^+$  +  $\text{Hg}^{2+}$ , **S1** +  $\text{Ag}^+$  +  $\text{Cr}^{3+}$ , and **S1** +  $\text{Ag}^+$  +  $\text{Mg}^{2+}$ , respectively.

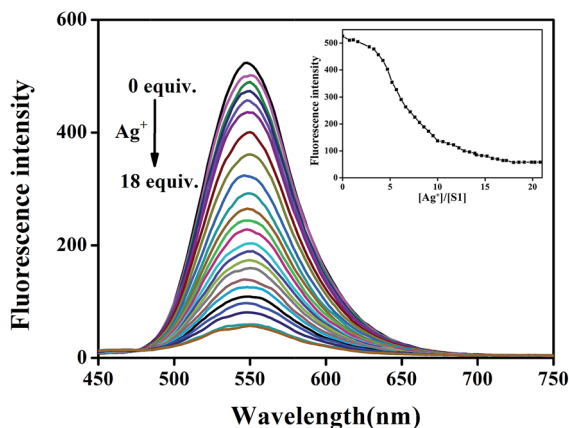


Fig. 3 Fluorescence spectra of **S1** (20  $\mu\text{M}$ ) in the presence of different concentrations of  $\text{Ag}^+$  (0–18 equiv.) in DMSO/ $\text{H}_2\text{O}$  (v:v = 1 : 1, buffered with HEPES pH = 7.2) solution. Inset: A plot of the fluorescence intensity depending on the concentration of  $\text{Ag}^+$  in the range from 0 to 18 equiv.

interactions in the sensor and confirms the coordination of the sensor and  $\text{Ag}^+$ . Based on the equation  $\text{LOD} = K \times \delta/S$ ,<sup>13</sup> the detection limits obtained from the UV-vis and the fluorescence spectra were  $8.75 \times 10^{-7}$  M and  $8.18 \times 10^{-9}$  M for silver ions, respectively.<sup>14</sup> This data indicates that the sensor can detect  $\text{Ag}^+$  at very low concentrations in the environment with high selectivity and sensitivity. This result also shows that **S1** has higher sensitivity for silver ions as compared to other reported  $\text{Ag}^+$  sensors (Table S1†). Therefore, **S1** can be used as a potential colorimetric and fluorescent sensor for  $\text{Ag}^+$  recognition.

Since the pH value of the environment around a chemosensor usually influences its detection toward target metal ions due to the protonation or deprotonation reaction of the sensor, the influence of pH value on the absorbance and emission bands of **S1** in a DMSO/water (1 : 1, v:v, buffered with HEPES pH

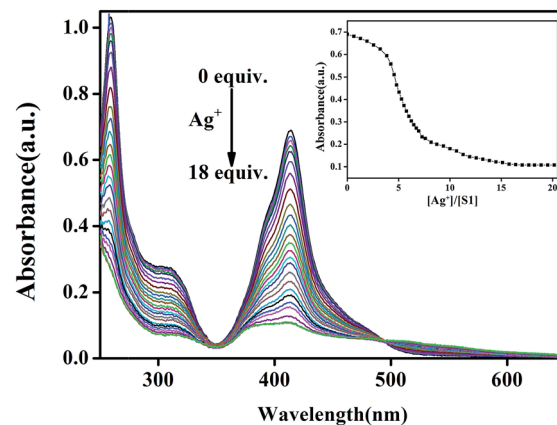


Fig. 4 Absorbance spectra of **S1** (20  $\mu\text{M}$ ) in the presence of different concentrations of  $\text{Ag}^+$  (0–18 equiv.) in the DMSO/ $\text{H}_2\text{O}$  (v:v = 1 : 1, buffered with HEPES pH = 7.2) solution. Inset: A plot of the variation in absorbance as a function of concentration of  $\text{Ag}^+$  in the range from 0 to 18 equiv.

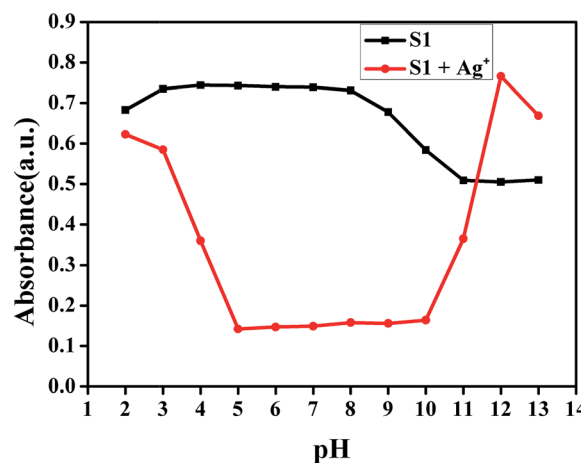


Fig. 5 pH response of **S1** and **S1**– $\text{Ag}^+$  in the DMSO/ $\text{H}_2\text{O}$  (v:v = 1 : 1; buffered with HEPES) solution.

= 7.2) solution has been investigated. As shown in Fig. 5 and S7,† when the pH increased from 5 to 10, the absorbance and emission values remained almost unchanged. These results indicated that  $\text{Ag}^+$  could be clearly detected *via* UV-vis and fluorescence spectral measurement using **S1** over a wide pH range.

The self-assembly and  $\text{Ag}^+$  recognition mechanism of the **S1** sensor were investigated using concentration titration, ESI-MS,  $^1\text{H}$  NMR titration, and DFT methods. To establish the supramolecular self-assembly mechanism, we performed the concentration titration in the absence and presence of different concentrations of **S1**. As shown in Fig. 6, the fluorescence intensity of the peak at 547 nm sharply increased with the addition of **S1**; this suggested that with the gradual increase in the concentration of **S1**, the self-assembled system was formed by  $\pi$ – $\pi$  stacking and H-bonding in the aqueous solution. Moreover, the XRD spectra (Fig. S8†) support the



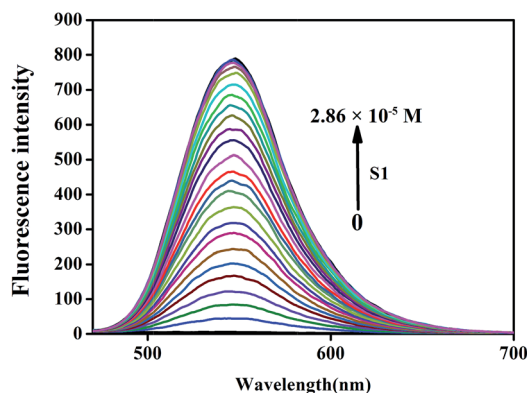


Fig. 6 Fluorescence spectra in the presence of different concentrations of **S1** ( $0$ – $2.86 \times 10^{-5}$  M) in the DMSO/H<sub>2</sub>O (v:v = 1 : 1, buffered with HEPES pH = 7.2) solution.

abovementioned competitive mechanism. The free sensor **S1** exhibits a peak at  $2\theta = 23.5^\circ$  corresponding to the  $d$  spacing of  $3.82 \text{ \AA}$ , which suggests that  $\pi$ – $\pi$  stacking exists. In addition, compared to **S1**–Ag, this peak disappeared; this is attributed to the coordination of  $\text{Ag}^+$  with the **S1** sensor. Based on all the abovementioned tests, we confirmed that **IM** self-assembly formed **S1** via  $\pi$ – $\pi$  stacking and H-bonding in the aqueous solution.

The reversibility of the sensor function was tested by the addition of  $\text{I}^-$  to the **S1**–Ag complex. With the alternative addition of  $\text{Ag}^+$  and  $\text{I}^-$  to the aqueous solution of the self-assembled **S1** sensor, the fluorescence emission of the tested solution exhibited alternating reviving and quenching processes (Fig. S9†). This off-on-off switching process was repeated several times. Therefore, the **S1** sensor can be considered a good ON–OFF fluorescence switch.

The 2 : 1 stoichiometry of the **S1** and  $\text{Ag}^+$  complex was further confirmed by the results of the ESI-MS studies. The free probe shows a main peak at  $m/z = 301.09$ , corresponding to  $[\text{IM} - \text{H}^+]$  (ESI-MS negative ion mode) (Fig. S14†), and the complex is confirmed by the appearance of a peak at  $m/z = 731.12$ , assignable to  $[2\text{IM} + \text{Ag}^+ + \text{H}_2\text{O} + \text{H}^+]$  (ESI-MS positive ion mode) (Fig. S15†). The Job plot between **S1** and  $\text{Ag}^+$  was implemented, demonstrating a 2 : 1 stoichiometry for **S1** and  $\text{Ag}^+$ , as shown in Fig. S16.†

The FTIR spectra of the receptor **IM** and its complex with  $\text{Ag}^+$  were obtained to examine the binding sites (Fig. S10†). In the FTIR spectrum of the free probe **IM**, the characteristic absorption band of **S1**– $\text{Ag}^+$  for N–H ( $3428 \text{ cm}^{-1}$ ) of the imidazole group was absent, and an obvious enhancement was observed for the C–N absorption bands from  $1322$  to  $1421 \text{ cm}^{-1}$ ; this confirmed the binding of **S1** with silver.

To gain more information about the complexation between **S1** and  $\text{Ag}^+$ , we performed an  $^1\text{H}$  NMR titration in the absence and presence of different concentrations of  $\text{Ag}^+$ . As shown in Fig. S11,† the  $^1\text{H}$  NMR titration of **S1** in DMSO- $d_6$  (10 mmol) with  $\text{Ag}^+$  in D<sub>2</sub>O (1 mol) established the stoichiometry and binding site towards the sensor response. Most interestingly, the N–H peak ( $\text{H}^1$ ) of the imidazole group in **IM** disappeared after the

addition of 2.0 equiv. of  $\text{Ag}^+$  to D<sub>2</sub>O;<sup>15</sup> this proved that **S1** was strongly bound with  $\text{Ag}^+$ . Moreover, the signal of the hydrogen atoms in the phenazine ( $\text{H}^2$ ,  $\text{H}^4$ ,  $\text{H}^5$ ,  $\text{H}^7$ , and  $\text{H}^8$ ) and thiazole ( $\text{H}^3$ ,  $\text{H}^6$ , and  $\text{H}^9$ ) rings showed a significant downfield shift; this suggested that the intermolecular  $\pi$ – $\pi$  stacking was destroyed after the addition of  $\text{Ag}^+$ , and it further caused the deshielding for the hydrogen protons and resulted in downfield shifts.

To further investigate the binding behavior of **S1** with  $\text{Ag}^+$  ions, we optimized the structure of **IM** and **IM**– $\text{Ag}^+$  complex by applying the B3LYP/6-31G(d, p) method in the gas phase using the Gaussian-09 computational code.<sup>16</sup> The optimized structures of **IM** and **IM**– $\text{Ag}^+$  are shown in Fig. S12 and S13,† respectively. The short N34–H49...N23 distance of  $2.041 \text{ \AA}$  indicates the presence of an intramolecular hydrogen bond in **IM**. Additionally, some of the relevant optimized geometric parameters are presented in Tables S2–S5.† The relevant occupied molecular orbital HOMO ( $-0.295 \text{ a.u.}$ ) of **IM** was localized mainly to the thiophene groups, whereas the unoccupied orbital LUMO ( $-0.227 \text{ a.u.}$ ) was localized over the phenazine and imidazole groups. The HOMO–LUMO energy gap (DE) for **IM** was found to be  $0.068 \text{ a.u.}$  (Fig. 7). On the other hand, upon interaction with  $\text{Ag}^+$ , the HOMO ( $-0.291 \text{ a.u.}$ ) and LUMO ( $-0.279 \text{ a.u.}$ ) were almost localized on the entire molecule, where the electron density was polarized toward the whole molecule. The HOMO–LUMO energy (DE) for **IM** with  $\text{Ag}^+$  was found to be  $0.012 \text{ a.u.}$  These results suggested that the fluorescence quenching was most probably attributed to the prevention of **IM** intramolecular charge transfer (ICT) by  $\text{Ag}^+$  (Scheme 1).

To investigate the practical application of the chemosensor **S1**, test strips were prepared by immersing filter paper in a DMSO/water (v:v = 1 : 1, buffered with HEPES pH = 7.2) solution of **S1** and then drying them in air. The test strips containing **S1** were utilized to sense  $\text{Ag}^+$  and other metal ions. As shown in Fig. 8, when  $\text{Ag}^+$  and other ions were added to the test kits, an obvious color change was only observed for the  $\text{Ag}^+$  solution under a 365 nm UV-lamp. The potential competitive

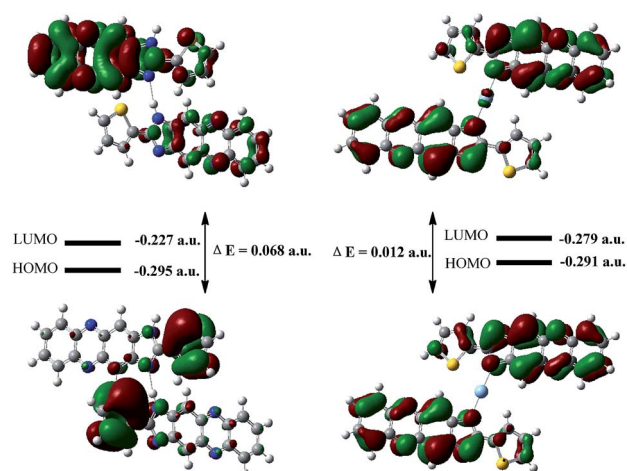


Fig. 7 DFT-optimized Frontier molecular orbitals and HOMO–LUMO energy gaps for **S1** (left) and **S1**– $\text{Ag}^+$  (right).



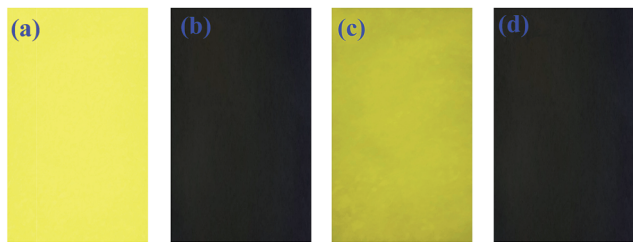


Fig. 8 Images of **S1** on test papers. (a) Only **S1**, (b) after immersion in DMSO/H<sub>2</sub>O (v:v = 1 : 1, buffered with HEPES pH = 7.2) solution with Ag<sup>+</sup>, (c) after immersion in DMSO/H<sub>2</sub>O (v:v = 1 : 1, buffered with HEPES pH = 7.2) solution with others cations, and (d) after immersion in DMSO/H<sub>2</sub>O (v:v = 1 : 1, buffered with HEPES pH = 7.2) solution with Ag<sup>+</sup> and other ions under irradiation at 365 nm.

ions did not influence the detection of Ag<sup>+</sup> by the test strips. Therefore, the test strips could conveniently detect Ag<sup>+</sup> in the solution.

## Conclusions

In summary, we developed a novel self-assembled supramolecular sensor **S1** that could recognize Ag<sup>+</sup> over other metal ions with significant UV-vis absorption and fluorescence quenching changes with highly selective and sensitive properties based on the competitive mechanism of supramolecular self-assembly. The obvious color changes and pronounced ON-OFF-type fluorescence signaling behavior can be seen by the naked eyes. The limit of detection for Ag<sup>+</sup> was as low as  $8.18 \times 10^{-9}$  M in an aqueous solution, which was lower than that in some previously reported research. We believe that the sensor will be regarded as an environmentally friendly material that can sense Ag<sup>+</sup> in an aqueous solution and make a great contribution to the development of silver ion sensors.

## Conflicts of interest

There are no conflicts to declare.

## Acknowledgements

This work was supported by the National Natural Science Foundation of China (NSFC) (21661028; 21574104; 21262032), the Natural Science Foundation of Gansu Province (1506RJZA273), and the Program for Changjiang Scholars and Innovative Research Team in University of Ministry of Education of China (IRT 15R56).

## Notes and references

- (a) T. Anand, D. Sivaraman, P. Anandh, D. Chellappa and S. Govindarajan, *Tetrahedron Lett.*, 2014, **55**, 671–675; (b) L. J. Bian, X. Ji and W. J. Hu, *J. Agric. Food Chem.*, 2014, **62**, 4870–4877.
- H.-T. Ratte, *Environ. Toxicol. Chem.*, 1999, **18**, 89–108.

- (a) C. M. Niemietz and S. D. Tyerman, *FEBS Lett.*, 2002, **531**, 443–447; (b) M. S. Pedroso, J. G. Bersano and A. Bianchini, *Environ. Toxicol. Chem.*, 2007, **26**, 2158–2165.
- X. B. Zhang, Z. X. Han, Z. H. Fang, G. L. Shen and R. Q. Yu, *Anal. Chim. Acta*, 2006, **562**, 210–215.
- M. Hu, J. Fan, J. Cao, K. Song, H. Zhang, S. Sun and X. Peng, *Analyst*, 2012, **137**, 2107–2111.
- (a) M. Hadioui, S. Leclerc and K. J. Wilkinson, *Talanta*, 2013, **105**, 15–19; (b) H. Yang, X. Liu, R. Fei and Y. Hu, *Talanta*, 2013, **116**, 548–553; (c) Z. Szigeti, A. Malon, T. Vigassy, V. Csokai, A. Grun, K. Wygladacz, N. Ye, C. Xu, V. J. Chebny, I. Bitter, R. Rathore, E. Bakker and E. Pretsch, *Anal. Chim. Acta*, 2006, **572**, 1–10; (d) G. Yan, Y. Wang, X. He, K. Wang, J. Su, Z. Chen and Z. Qing, *Talanta*, 2012, **94**, 178–183.
- (a) B. Zhang, J. Sun, C. Bi, G. Yin, L. Pu, Y. Shi and L. Sheng, *New J. Chem.*, 2011, **35**, 849–853; (b) Z. Xu, S. Zheng, J. Yoon and D. R. Spring, *Analyst*, 2010, **135**, 2554–2559; (c) H.-H. Wang, L. Xue, Y.-Y. Qian and H. Jiang, *Org. Lett.*, 2010, **12**, 292–295; (d) C. Huang, A. Ren, C. Feng and N. Yang, *Sens. Actuators, B*, 2010, **151**, 236–242; (e) T. Chen, W. Zhu, Y. Xu, S. Zhang, X. Zhang and X. Qian, *Dalton Trans.*, 2010, **39**, 1316–1320; (f) C. S. Park, J. Y. Lee, E.-J. Kang, J.-E. Lee and S. S. Lee, *Tetrahedron Lett.*, 2009, **50**, 671–675; (g) L. Liu, D. Zhang, G. Zhang, J. Xiang and D. Zhu, *Org. Lett.*, 2008, **10**, 2271–2274; (h) S. Iyoshi, M. Taki and Y. Yamamoto, *Inorg. Chem.*, 2008, **47**, 3946–3948; (i) C. Huang, X. Peng, Z. Lin, J. Fan, A. Ren and D. Sun, *Sens. Actuators, B*, 2008, **133**, 113–117; (j) R.-H. Yang, W.-H. Chan, A. W. M. Lee, P.-F. Xia and H.-K. Zhang, *J. Am. Chem. Soc.*, 2003, **125**, 2884–2885; (k) C. Liu, S. Huang, H. Yao, S. He, Y. Lu, L. Zhao and X. Zeng, *RSC Adv.*, 2014, **4**, 16109–16114; (l) A. Affrose, S. D. S. Parveen, B. S. Kumar and K. Pitchumani, *Sens. Actuators, B*, 2015, **206**, 170–175; (m) Q. Lin, Q. P. Yang, B. Sun, T.-B. Wei and Y.-M. Zhang, *Chin. J. Chem.*, 2014, **32**, 1255–1258; (n) Y. Li, H. Yu, G. Shao and F. Gan, *J. Photochem. Photobiol., A*, 2015, **301**, 14–19.
- (a) C. Liu, S. Huang, H. Yao, S. He, Y. Lu, L. Zhao and X. Zeng, *RSC Adv.*, 2014, **4**, 16109–16114; (b) Y.-T. Wu, J.-L. Zhao, L. Mu, X. Zeng, G. Wei, C. Redshaw and Z. Jin, *Sens. Actuators, B*, 2017, **252**, 1089–1097; (c) C. Chen, H. Liu, B. Zhang, Y. Wang, K. Cai, Y. Tan, C. Gao, H. Liu, C. Tan and Y. Jiang, *Tetrahedron*, 2016, **72**, 3980–3985; (d) Y. Jiang, W. Kong, Y. Shen and B. Wang, *Tetrahedron*, 2015, **71**, 5584–5588; (e) T.-B. Wei, H. L. Zhang, W. T. Li, W. J. Qu, J. X. Su, Q. Lin, Y. M. Zhang and H. Yao, *Chin. J. Chem.*, 2017, **35**, 1311–1316.
- (a) F. Qu, J. Liu, H. Yan, L. Peng and H. Li, *Tetrahedron Lett.*, 2008, **49**, 7438–7441; (b) X. Liu, X. Yang, Y. Fu, C. Zhu and Y. Cheng, *Tetrahedron*, 2011, **67**, 3181–3186; (c) F. Li, F. Meng, Y. Wang, C. Zhu and Y. Cheng, *Tetrahedron*, 2015, **71**, 1700–1704; (d) Y. Wang, H. Q. Chang, W.-N. Wu, X.-L. Zhao, Y. Yang, Z. Q. Xu, Z. H. Xu and L. Jia, *Sens. Actuators, B*, 2017, **239**, 60–68.
- (a) X. H. Li, X. H. Gao, W. Shi and H. M. Ma, *Chem. Rev.*, 2014, **114**, 590–659; (b) Z. Q. Guo, S. Park, J. Yoon and



- I. Shin, *Chem. Soc. Rev.*, 2014, **43**, 16–29; (c) K. Zscharnack, T. Kreisig, A. A. Prasse and T. Zuchner, *Anal. Chim. Acta*, 2014, **834**, 51–57; (d) S. Goswami, A. K. Das, A. Manna, A. K. Maity, P. Saha, C. K. Quah, H. Fun and H. A. Abdel-Aziz, *Anal. Chem.*, 2014, **86**, 6315–6322; (e) R. Kramer, *Angew. Chem., Int. Ed.*, 1998, **37**, 772–773; (f) L. Fabbri and A. Poggi, *Chem. Soc. Rev.*, 1995, **24**, 197–202.
- 11 (a) B. B. Shi, P. Zhang, T.-B. Wei, H. Yao, Q. Lin and Y.-M. Zhang, *Chem. Commun.*, 2013, **49**, 7812–7814; (b) Q. Lin, T. T. Lu, J. C. Lou, G. Y. Wu, T.-B. Wei and Y.-M. Zhang, *Chem. Commun.*, 2015, **51**, 12224–12227; (c) Q. Lin, F. Zheng, L. Liu, P. P. Mao, Y. M. Zhang, H. Yao and T. B. Wei, *RSC Adv.*, 2016, **6**, 111928–111933; (d) Q. Lin, T. T. Lu, X. Zhu, T. B. Wei, H. Li and Y. M. Zhang, *Chem. Sci.*, 2016, **7**, 5341–5346; (e) Q. Lin, T. T. Lu, X. Zhu, B. Sun, Q. P. Yang, T. B. Wei and Y. M. Zhang, *Chem. Commun.*, 2015, **51**, 1635–1638; (f) Q. Lin, P. P. Mao, L. Liu, Y. M. Zhang, H. Yao and T. B. Wei, *RSC Adv.*, 2017, **7**, 11206–11210; (g) Q. Lin, B. Sun, Q. P. Yang, Y. P. Fu, X. Zhu, T. B. Wei and Y. M. Zhang, *Chem.–Eur. J.*, 2014, **20**, 11457–11462; (h) X. B. Cheng, H. Li, F. Zheng, Q. Lin, H. Yao, Y. M. Zhang and T. B. Wei, *RSC Adv.*, 2016, **6**, 20987–20993.
- 12 (a) Y. X. Zhao, Y. Y. Liu, Z. Y. Wang, W. H. Xu, B. Liu, J. H. Su, B. Wu and X. J. Yang, *Chem. Commun.*, 2015, **51**, 1237–1239; (b) C. G. Wang, G. Li and Q. C. Zhang, *Tetrahedron Lett.*, 2013, **54**, 2633–2636; (c) Q. L. Xu, C. H. Heo, G. G. Kim, H. W. Lee, H. M. Kim and J. Y. Yoon, *Angew. Chem., Int. Ed.*, 2015, **54**, 4890–4894.
- 13 M. H. Yang, P. Thirupathi and K. H. Lee, *Org. Lett.*, 2011, **13**, 5028–5031.
- 14 (a) L. Yang, X. Li, J. Yang, Y. Qu and J. Hua, *ACS Appl. Mater. Interfaces*, 2013, **5**, 1317–1326; (b) F. Zheng, F. Zeng, C. Yu, X. Hou and S. Wu, *Chem.–Eur. J.*, 2013, **19**, 936–942.
- 15 M. Shellaiah, M. V. R. Raju, A. Singh, H.-C. Lin, K.-H. Wei and H.-C. Lin, *J. Mater. Chem. A*, 2014, **2**, 17463–17476.
- 16 M. J. Frisch, G. W. Trucks, H. B. Schlegel, G. E. Scuseria, M. A. Robb, J. R. Cheese-man, J. A. Montgomery Jr, T. Vreven, K. N. Kudin, J. C. Burant, J. M. Millam, S. S. Iyengar, J. Tomasi, V. Barone, B. Mennucci, M. Cossi, G. Scalmani, N. Rega, G. A. Petersson, H. Nakatsuji, M. Hada, M. Ehara, K. Toyota, R. Fukuda, J. Hasegawa, M. Ishida, T. Nakajima, Y. Honda, O. Kitao, H. Nakai, M. Klene, X. Li, J. E. Knox, H. P. Hratchian, J. B. Cross, V. Bakken, C. Adamo, J. Jaramillo, R. Gomperts, R. E. Stratmann, O. Yazyev, A. J. Austin, R. Cammi, C. Pomelli, J. W. Ochterski, P. Y. Ayala, K. Morokuma, G. A. Voth, P. Salvador, J. J. Dannenberg, V. G. Zakrzewski, S. Dapprich, A. D. Daniels, M. C. Strain, O. Farkas, D. K. Malick, A. D. Rabuck, K. Raghavachari, J. B. Foresman, J. V. Ortiz, Q. Cui, A. G. Baboul, S. Clifford, J. Cioslowski, B. B. Ste-fanov, G. Liu, A. Liashenko, P. Piskorz, I. Komaromi, R. L. Martin, D. J. Fox, T. Keith, M. A. Al-Laham, C. Y. Peng, A. Nanayakkara, M. Challacombe, P. M. W. Gill, B. John-son, W. Chen, M. W. Wong, C. Gonzalez and J. A. Pople, *Gaussian 09W*, Gaussian, Inc., Wallingford, CT, 2009.

